DETERMINATION OF ISOMERIC RATIOS IN NEUTRON-RICH TIN ISOTOPES PRODUCED IN PROJECTILE FRAGMENTATION*

F. von Spee [a], G. Georgiev [a], S. Go [b], M. Niikura [b], K. Stoychev [a,c], H. Baba [b], D. Balabanski [e], S.R. Ban [e], D. Choudhury [l], A. Coman [f], C. Costache [f], J.-M. Daugas [d], L.M. Fraile [g], N. Fukuda [b], Y. Fukuzawa [b], G. Garcia de Lorenzo [g], Y. Ichikawa [h], Y. Ichinohe [b], N. Imai [i], D. Kalaydjieva [c], T. Kato [b], N. Kitamura [i], A. Kusoglu [e], G. Li [j], Z. Liu [j], M. Matsuda [k], H. Matsufuji [h], R. Matsui [h], Y. Matsuo [b], S. Michimasa [b], C. Mihai [f], Y. Mizuno [i], M. Mochizuki [b], S. Motomura [b], M. Mukai [b], H. Nishibata [h], A. Odahara [k], S. Ohno [b], S. Pascu [f], S. Shimano [b], K. Shimizu [b], Y. Shimizu [b], M. Si [j], H. Suzuki [b], S. Takahashi [b], A. Takamine [h], H. Takeda [b], Y. Togano [b], A. Turturica [f], G. Turturica [e], H. Ueno [b], S. Ujeniuc [f], Y. Yamamoto [i], M. Yoshimoto [b]

[a] Université Paris-Saclay, CNRS/IN2P3, IJCLab, Orsay, France
[b] RIKEN Nishina Center, Wako, Saitama, Japan
[c] University of Guelph, Department of Physics, Guelph, Canada
[d] Institut Laue-Langevin, Grenoble, France
[e] Extreme Light Infrastructure — Nuclear Physics, IFIN-HH, Măgurele, Romania
[f] Horia Hulubei Inst. of Physics and Nuclear Engineering, Măgurele, Romania
[g] Universidad Complutense de Madrid, Madrid, Spain
[h] Department of Physics, Kyushu University, Japan
[i] Center for Nuclear Study, University of Tokyo, Japan
[j] Institute of Modern Physics, Chinese Academy of Sciences, China
[k] Department of Physics, Osaka University, Japan
[l] Dep. of Physics, Indian Institute of Technology Ropar, Rupnagar, Punjab, India

Received 15 November 2025, accepted 22 January 2026, published online 31 March 2026

The beam composition of a tertiary ^{130}Sn beam that was produced in projectile fragmentation is analyzed. This allows, in a first step, to identify contaminants in the beam and, in a second step, to determine isomeric ratios for different isotopes present in the beam. The results help to understand the process of projectile fragmentation and to plan future experiments that involve similar reactions.

DOI:10.5506/APhysPolBSupp.19.1-A21

* Presented at the XXXVIII Mazurian Lakes Conference on Physics, Piaski, Poland, August 31–September 6, 2025.

1. Introduction

With the development of rarer and rarer isotope beams, the desire to control other parameters of the beam has also increased. Ichikawa *et al.* [1] were able to show how to control the spin orientation of beams produced in projectile fragmentation. Such beams can be used to perform Time Dependent Perturbed Angular Distribution (TDPAD) (see *e.g.* [2]) measurements where a spin alignment is necessary for a successful measurement. Another important aspect of beams produced in projectile fragmentation, that is also relevant for TDPAD experiments, is the population of isomeric states. The population of isomeric states relative to the population of the ground state is known as the isomeric ratio. The populated isomeric states also represent the states of interest for a TDPAD measurement that is suited for the determination of magnetic moments of states with lifetimes in the microsecond regime. The determination of isomeric ratios is hence of interest for TDPAD measurements.

2. Experiment

A TDPAD measurement was performed at the RIKEN Nishina Center to measure the g factor of the 10^+ state in ^{130}Sn. To this aim, a secondary ^{132}Sn beam was produced in the fragmentation of 345 MeV/u ^{238}U on a ^{9}Be target with 3 mm thickness. This secondary beam with a beam energy of about 160 MeV/u impinged on a wedge-shaped aluminum target of 3 mm thickness. From the resulting projectile fragmentation, a tertiary ^{130}Sn beam was extracted. The tertiary ^{130}Sn beam was momentum selected as described in [1] and then passed through a plastic detector before it was implanted in a copper host, situated at the center of a vacuum chamber. The target chamber was surrounded by four planar High Purity Germanium (HPGe) detectors each of which was placed at a 90° angle with respect to its neighboring detectors. The experiment was conducted for about 72 h with an average beam intensity of the tertiary beam of about 150 particles per second. Before the experiment, a ^{133}Ba source was placed at the center of the chamber to determine the detector efficiencies. In the following analysis, the beam composition of the tertiary beam is analyzed. Contaminations of the ^{130}Sn beam are identified and isomeric ratios are calculated.

3. Data analysis

It is useful to distinguish three different time realms with respect to the detection of a beam particle passing through the plastic detector: The *prompt* window contains events that happen within 100 ns of the detection of a beam particle in the plastic detector, where γ-ray spectra are typically dominated by the atomic flash of the heavy ions stopping in the host ma-

terial. The *delayed* window contains events that happen not in the prompt window, but within 10 μs of the detection of a beam particle in the plastic detector, typically dominated by the decays of isomeric states. The length of the delayed window is about six times the half-life of the 10^+ isomer in ^{130}Sn of 1.6 μs [3]. Since the half-life is, on the other hand, significantly larger than the prompt window, most γ-ray transitions following the decay of the 10^+ isomer are observed in the delayed spectrum. Such a delayed spectrum is shown in Fig. 1, where the transitions of interest in ^{130}Sn, the $10^+ \rightarrow 8^+$ (96 keV) [3] and $8^+ \rightarrow 7^-$ (392 keV) [3] transitions are clearly visible. Lastly, *uncorrelated* events are collected outside of prompt and delayed windows, and are dominated by transitions that originate from β decays of implanted nuclei (see Fig. 2). Since many γ rays following β decays observed in uncorrelated spectra are very well known, these transitions are useful not only for beam composition analysis, but also for improving the detection efficiency calibration.

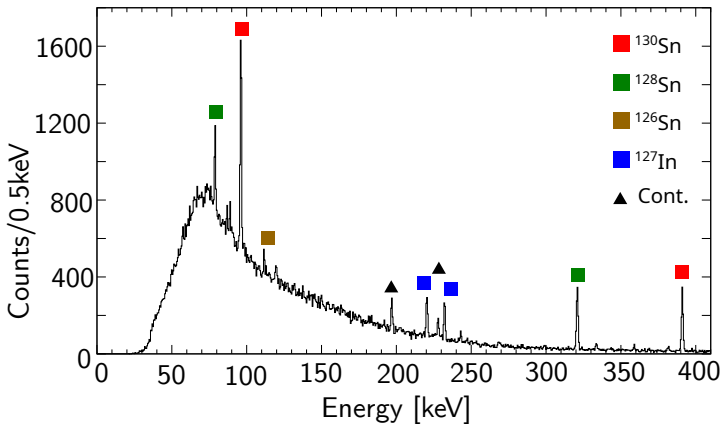

Fig. 1. (Color online) Summed delayed spectra of all four HPGe detectors. Transitions following an isomeric decay of the implanted beam particles are shown in colored squares. Contaminating γ-ray transitions that stem from other sources are marked with a black triangle.

3.1. Efficiency calibration

For a quantitative analysis of the spectra, it is necessary to determine the absolute γ-ray detection efficiency that depends on the γ-ray energy. The detection efficiency was determined both using data from the ^{133}Ba source measurement and in-beam data. In the case of the ^{133}Ba source, absolute efficiencies were determined using the known γ-ray intensities of the ^{133}Ba source, the activity of the source, and the measurement time. In order to extract absolute efficiencies from in-beam data, γ-ray intensities

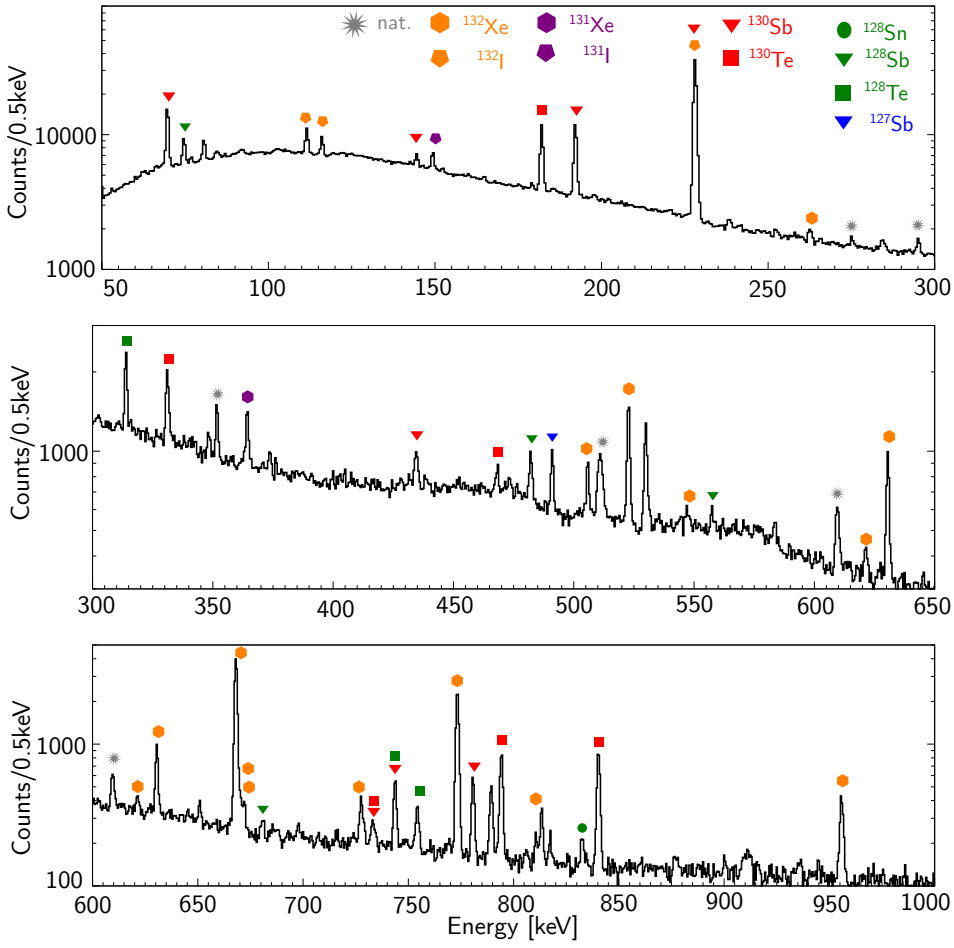

Fig. 2. Uncorrelated γ-ray spectrum during the TDPAD experiment. Since the line density is relatively high, only the spectrum recorded in the HPGe detector with the best energy resolution is shown.

of transitions that occurred after β decays were considered. The intensity $I_a(\gamma_1)$ of a γ-ray transition γ_1 with energy E_1 observed in the detector a is given by

$$I_a(\gamma_1) = A\, p(\gamma_1)\, W_a(E_1)\,, \tag{1}$$

where $W_a(E)$ is the probability that a γ ray with energy E_1 emitted from the source is detected in the detector a, $p(\gamma_1)$ is the probability that a γ ray γ_1 is emitted after β decay, and A is the β-decay activity.

A similar relation can be found for the coincidence intensity $I_{ab}([\gamma_1, \gamma_2])$ of two coincident γ-ray transitions $\gamma_{1,2}$ in two detectors a, b. By measuring the intensity $I_{\mathrm{sum}}(\gamma_2)$ and the coincidence intensity $I_{\mathrm{sum}}([\gamma_1, \gamma_2])$, it is possible to extract the absolute efficiency W_{sum} at the energy E_1

$$W_{\mathrm{sum}}(E_1) = \frac{4}{3} \frac{I_{\mathrm{sum}}([\gamma_1, \gamma_2])}{I_{\mathrm{sum}}(\gamma_2)} \frac{p(\gamma_2)}{p([\gamma_1, \gamma_2])}\,, \tag{2}$$

where the factor $4/3$ takes into account that the setup has four detectors and that the quantities I_{sum} are summed over all detectors or detector pairs. With this formula, absolute efficiencies were calculated for the 331–182–793 keV and 780–192 keV cascades following the β decays ^{130}Sb $\rightarrow$ ^{130}Te and ^{130}Sn $\rightarrow$ ^{130}Sb, respectively.

Absolute efficiencies from both the source measurement and the in-beam measurement are shown in Fig. 3. While efficiency values determined in the source measurement have a relatively small uncertainty, efficiency values determined with in-beam data have a relatively large uncertainty caused mainly by the low statistics of the observed γ–γ coincidence intensities. The data were interpolated using the sum of two exponential functions. Since there is only one determined efficiency for a γ-ray energy larger than 400 keV and since that efficiency was determined using in-beam data, the uncertainty of interpolated absolute efficiencies of γ-rays with energies greater than 400 keV is relatively large.

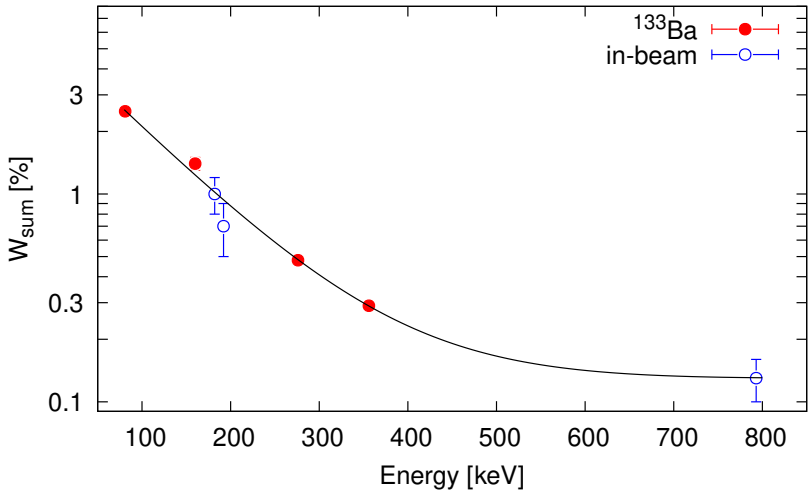

Fig. 3. (Color online) Absolute efficiencies W_{sum} for different γ-ray energies determined using data from the ^{133}Ba source measurement (full dots/red) and using in-beam data (empty dots/blue). A fitted interpolation function consisting of the sum of two exponential functions is shown in black.

3.2. Quantitative analysis of uncorrelated spectra

The uncorrelated spectra (see Fig. 2) contain transitions following the decay of beam particles whose lifetimes are much longer than the delayed window ($T_{1/2} \gg 10$ μs). These include the observed transitions that follow β decays of nuclei with masses 130, 128 and 127 (see Fig. 4), but also the 832 keV transition following the isomeric decay of the 7^- state in ^{128}Sn, which has a lifetime of about 9 s. In addition, transitions stemming from natural radioactivity — mainly from ^{222}Rn — can be seen. Finally, since the target had been briefly irradiated with a relatively intense ^{132}Sn beam prior to the experiment, the spectra are dominated by transitions following longer-lived β decays ($T_{1/2} \gtrsim 1$ h) of nuclei with mass 132 or 131 (see Fig. 4). Unfortunately, some of the observed transitions remain unidentified, most notably a transition at around 530 keV.

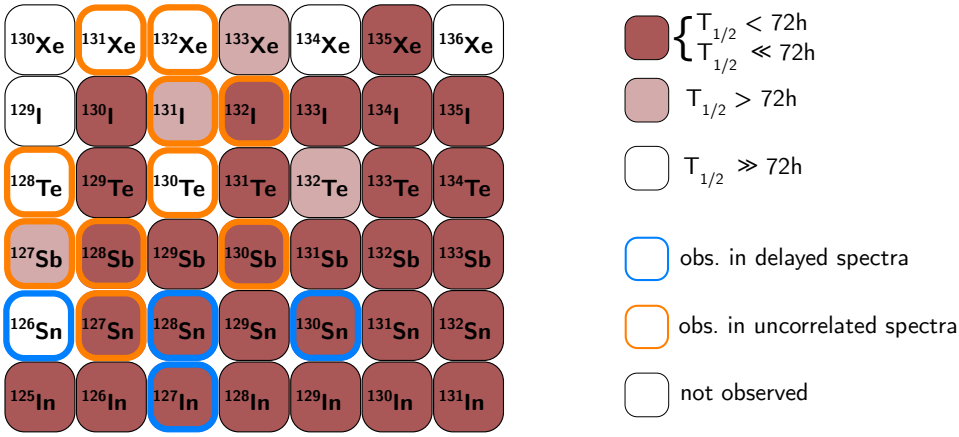

Fig. 4. Qualitative overview of the different nuclei observed through delayed and uncorrelated γ-ray spectroscopy during the TDPAD experiment.

The measured intensities of the observed γ-ray transitions can be compared to the known intensities of γ-ray transitions following β decays with masses 130 [3], 128 [4], and 127 [5]. This allows us to calculate the number of the associated β decays that occurred during the experiment. For short-lived species ($T_{1/2} \ll 72$ h), this number will correspond to the number of implanted ions of the parent nuclei. The same calculation is possible for the isomeric decay of the 7^- state in ^{128}Sn. From the results of these calculations presented in Table 1, it becomes clear that ^{130}Sn was the main component of the used tertiary beam. About $1.1(2) \times 10^7$ ^{130}Sn ions have been implanted during the experiment. However, also about $3.4(10) \times 10^6$ ^{128}Sn ions and $2.8(11) \times 10^6$ ^{127}In ions were present in the beam.

Table 1. Determination of the number # of different parent decays that occurred during the TDPAD experiment. Half-lives ($T_{1/2}$) are given in minutes, transition energies E_γ in keV, absolute γ-ray intensities I_γ and absolute efficiencies $W_{\rm sum}(E)$ in percent. The details on decaying parent states, including spin and parity, half-life, and the absolute γ-ray intensity, were taken from Refs. [3–8].

Decay	$T_{1/2}$	E_γ	I_γ	$W_{\rm sum}(E)$	$I_\gamma^{\rm obs}$ [10^3]	# [10^6]
^{130}Sn, $0^+ \rightarrow {}^{130}$Sb	3.7	192	67(2)	0.9(3)	60(1)	10(3)
^{130}Sn, $0^+ \rightarrow {}^{130}$Sb	3.7	780	56(2)	0.13(4)	5.2(1)	7(2)
^{130}Sn, $7^- \rightarrow {}^{130}$Sb	1.7	145	23(3)	1.4(4)	8.3(3)	2.6(8)
^{130}Sn, $7^- \rightarrow {}^{130}$Sb	1.7	733	23(3)	0.13(4)	1.1(1)	3.7(12)
^{130}Sb $\rightarrow {}^{130}$Te [1]	— [1]	793	100(5)	0.13(4)	9.1(1)	7(2)
^{130}Sb, $8^- \rightarrow {}^{130}$Te	40	330	78(4)	0.33(10)	9.8(2)	3.8(11)
^{128}Sn, $0^+ \rightarrow {}^{128}$Sb	59	482	59(6)	0.17(7)	3.4(1)	3.3(13)
^{128}Sn, $0^+ \rightarrow {}^{128}$Sb	59	681	16(2)	0.13(4)	0.75(10)	3.6(14)
^{128}Sb, $5^+ \rightarrow {}^{128}$Te	10	314	88(5)	0.37(11)	10.0(5)	3.1(9)
^{128}Sb, $5^+ \rightarrow {}^{128}$Te	10	754	96(5)	0.13(4)	2.5(1)	2.0(8)
^{127}Sn, $3/2^+ \rightarrow {}^{127}$Sb	4	491	97(19)	0.17(7)	4.7(2)	2.8(11)
^{128}Sn, $7^- \rightarrow {}^{128}$Sn [2]	0.1	832	100	0.13(3)	0.85(15)	0.7(2)

[1] The 793 keV transition is present in both possible β decays of ^{130}Sb with the same intensity.

[2] While all other decays presented in this table are β decays, the 7^- state in ^{128}Sn decays isomerically.

It is observed that the number of ^{130}Sb $\rightarrow$ ^{130}Te decays is slightly smaller than the number of ^{130}Sn $\rightarrow$ ^{130}Sb decays, and also that the number of ^{128}Sb $\rightarrow$ ^{128}Te decays is slightly smaller than the number of ^{128}Sn $\rightarrow$ ^{128}Sb decays, although the two yields would be expected to be approximately equal. This discrepancy may possibly be attributed to short interruptions during the experiment. Furthermore, the number of beam particles observed in the plastic detector, 3.7×10^7, is about twice as large as the previously calculated number of implanted ions, $1.7(2) \times 10^7$. Possible reasons for this discrepancy again include short measurement interruptions, as well as the presence of unobserved, stable beam contaminants.

3.3. Quantitative analysis of delayed spectra

The delayed spectra (see Fig. 1) show γ-ray transitions following the decay of isomers with lifetimes in the microsecond range. Since the delayed spectra are correlated with the detection of a beam particle passing through

the plastic detector, the nucleus in the isomeric state must have been present in the beam. If the lifetime of the isomer is much longer than 100 ns but much shorter than 10 μs, the total number of beam nuclei in the isomeric states can be determined from the corresponding observed γ-ray intensities. The results of the calculation are shown in Table 2. For ^{128,130}Sn and ^{127}In, two γ-ray transitions can be observed following the decay of the isomer. The total number of nuclei in the isomeric state calculated from both transitions agrees well for ^{130}Sn and ^{127}In, but not for ^{128}Sn. This discrepancy is likely related to the efficiency W_{sum} (79 keV), which may be overestimated. At such low γ-ray energies, absorption in surrounding materials, for example, in the target chamber, becomes significant. Consequently, the value derived from the 321 keV transition is considered more reliable.

Table 2. Analysis of the intensity of observed γ-ray transitions I_γ^{obs} following an isomeric decay to calculate the number # of implanted nuclei in the respective isomeric state. Transition energies E_γ are given in keV, isomeric half-lives $T_{1/2}$ in μs and absolute efficiencies $W_{\mathrm{sum}}(E)$ in percent. The details on the isomeric states, including transition energies, half-lives, spins and parities, and internal conversion coefficients α_C are adopted from [3–8].

E_γ	Nucleus	J^π_{isomer}	$T_{1/2}$	α_C	$W_{\mathrm{sum}}(E)$	I_γ^{obs}	# [10^5]
97	^{130}Sn	10^+	1.6	1.8	2.2(7)	2500(100)	3.2(10)
391	^{130}Sn	10^+	1.6	0.004	0.24(7)	840(30)	3.5(10)
79	^{128}Sn	10^+	2.9	3.7	2.6(8)	780(70)	1.4(4)
321	^{128}Sn	10^+	2.9	0.007	0.36(10)	900(30)	2.5(8)
233	^{127}In	$^{29}/_2{}^+$	9	0.02	0.6(2)	480(30)	0.8(2)
221	^{127}In	$^{29}/_2{}^+$	9	0.02	0.7(2)	550(30)	0.8(2)
112	^{126}Sn	7^-	6.1	1.1	1.9(6)	230(50)	0.28(8)

The isomeric ratios for the 10^+ and 7^- isomers in ^{128,130}Sn are calculated by combining the information from uncorrelated and delayed spectra. The number of nuclei in the ground state and 7^- isomer are given in Table 1, and the number of nuclei in the 10^+ isomer in Table 2. It should be noted that in ^{128}Sn, the 10^+ isomer decays via the 7^- isomer to the ground state, while in ^{130}Sn, the 10^+ isomer populates the 7^- isomer, which then decays directly by β decay. This has been taken into account in the calculation of the isomeric ratios that are presented in Table 3. The resulting values demonstrate that the determined isomeric ratios for ^{128}Sn and ^{130}Sn produced in this projectile fragmentation reaction show similarities. In both cases, the ground state has the highest population, while 7^- and 10^+ together have about a third of the population of the ground state.

Table 3. Isomeric ratios determined in ^{130,128}Sn and ^{127}In. The ratios are normalized to the number of observed ground states. Since the number of implanted ^{127}In is unknown, only the number of decays to ^{127}Sb is known, a lower limit is given for the isomeric ratio.

^{130}Sn		^{128}Sn		^{127}In	
Isomer	Ratio	Isomer	Ratio	Isomer	Ratio
0^+_g	100(30)	0^+_g	100(40)	total	100
7^-	32(10)	7^-	17(5)	$^{29}/_{2}^+$	≥ 4
10^+	4(3)	10^+	9(3)		

For the $^{29}/_{2}^+$ isomer in ^{127}In, only a lower limit of the isomeric ratio is given, since the number of nuclei in the ground state is determined only indirectly using the ^{127}Sn $\rightarrow$ ^{127}Sb decay and because the half-life of the isomer is relatively long compared to the size of the delayed window.

The isomeric ratios determined here are the isomeric ratios after implantation and prompt window; the isomers partially decay already in-flight, since the flight time from the secondary target to the implantation is around 300 ns.

4. Summary

In this work, the beam composition of a tertiary ^{130}Sn beam which was produced in projectile fragmentation of ^{132}Sn on aluminum was analyzed. Beam contaminants of ^{126,128}Sn and ^{127}In were identified. In ^{128,130}Sn, the isomeric ratios of the 7^- and 10^+ isomers were determined. Although the results carry relatively large uncertainties, mainly due to uncertainties in the absolute γ-ray efficiencies, they improve our understanding of the projectile fragmentation process and can be used to plan future experiments.

This work was supported by the Romanian Ministry of Research and Innovation under the research contract PN 23 21 01 06 of the ELI-RO program funded by the Institute of Atomic Physics, Măgurele, Romania, contract numbers ELI-RO/RDI/2024 002 and ELI-RO/RDI/2024 007.

REFERENCES

[1] Y. Ichikawa *et al.*, *Nature Phys.* **8**, 918 (2012).

[2] R. Neugart, G. Neyens, «Nuclear Moments», *Springer*, Berlin, Heidelberg 2006, pp. 135–189.

[3] B. Singh, *Nucl. Data Sheets* **93**, 33 (2001).
[4] Z. Elekes, J. Timar, *Nucl. Data Sheets* **129**, 191 (2015).
[5] A. Hashizume, *Nucl. Data Sheets* **112**, 1647 (2011).
[6] H. Iimura, J. Katakura, S. Ohya, *Nucl. Data Sheets* **180**, 1 (2022).
[7] Y. Khazov, A. Rodionov, S. Sakharov, B. Singh, *Nucl. Data Sheets* **104**, 497 (2005).
[8] Y. Khazov, I. Mitropolsky, A. Rodionov, *Nucl. Data Sheets* **107**, 2715 (2006).